Jet-Cooled 2-Aminopyridine Dimer: Conformers and Infrared Vibrational Spectra

Philipp Ottiger, Jann A. Frey, Hans-Martin Frey, and Samuel Leutwyler*

Departement für Chemie and Biochemie, Universität Bern, Freiestrasse 3, CH-3012 Bern, Switzerland

Received: December 23, 2008; Revised Manuscript Received: February 18, 2009

The 2-aminopyridine dimer, $(2AP)_2$, is linked by two N−H···N hydrogen bonds, providing a model for the Watson−Crick configurations of the adenine or cytosine self-dimers. Structure optimization of $(2AP)_2$ at the MP2 level with the aug-cc-pVQZ basis set establishes the existence of two nearly degenerate conformers with C_i and C_2 symmetry. Adding complete basis set extrapolation and ΔCCSD(T) corrections gives binding energies $D_e = 10.70$ and 10.72 kcal/mol, respectively. Both isomers are chiral, each giving rise to a pair of enantiomers. The potential energy surface of $(2AP)_2$ is calculated along the 2AP amino flip coordinates, revealing a 4-fold minimum low-energy region with a planar C_{2h} symmetric and four asymmetric transition structures. The mass-selective resonant two-photon ionization (R2PI) spectra of supersonically cooled $(2AP)_2$ were remeasured. Three different species (A−C) were separated and characterized by UV/UV depletion spectroscopy and by infrared (IR) depletion spectroscopy in the 2600−3800 cm^{-1} range. The R2PI and IR spectra of species A and B are very similar, in agreement with the prediction of two conformers of $(2AP)_2$. The IR bands are assigned to the H-bonded N−H_b stretch, the N−H_2 bend overtone, and the free N−H_f stretch of $(2AP)_2$, based on the calculated IR spectra, thereby extending and correcting previous assignments. Conformer A is tentatively assigned as the C_2 conformer. The UV spectrum of species C is very different from those of A and B, its IR spectrum exhibiting additional O−H stretching bands. C is assigned to the $(2AP)_2 \cdot H_2O$ cluster, based on the agreement of its IR spectrum with calculated IR spectra. Complete dissociation into the $(2AP)_2^+$ ion occurs upon ionization.

I. Introduction

2-Aminopyridine (2AP) is a structural mimic of the Watson−Crick hydrogen-bonding site of adenine, offering both an N−H donor and aromatic N acceptor group.[1−4] 2AP, the dimer $(2AP)_2$, and the 2AP·2-pyridone heterodimer have therefore been widely employed as models for doubly hydrogen-bonded DNA base pairs in the gas phase.[5−10]

Kydd and Mills showed by microwave spectroscopy that the NH_2 group of 2AP is nonplanar with an angle of ∼32° between the H−N−H bisector and its projection in the plane of the pyridine frame.[1] Also, one hydrogen is 0.7 Å closer to the ring plane, providing evidence for an intramolecular hydrogen bond.[1] Borst et al. measured the high-resolution, rotationally resolved $S_1 \leftarrow S_0$ spectrum of 2AP and determined the corresponding $S_1 \leftarrow S_0$ transition moment direction, S_1 state rotational constants, and inertial defect ΔI.[4] Hager et al. have undertaken pioneering studies of a number of van der Waals and hydrogen-bonded complexes and clusters of 2AP[2,11,12] and $(2AP)_2$,[3] using two-color resonant two-photon ionization (2C-R2PI) spectroscopy and fluorescence lifetime measurements.[3] They considered the symmetric hydrogen-bonded arrangement of $(2AP)_2$ shown in the following scheme. They rationalized the large spectral shift of $(2AP)_2$ relative to the 2AP monomer of $\delta\nu = -1668$ cm^{-1} in terms of a stabilization of the S_1 excited-state by 4.8 kcal/mol relative to the ground state.[3]

The R2PI and mass-analyzed threshold ionization (MATI) spectra have been recorded for 2AP,[13,14] its mono- and dideuterated isotopomers, and the 2AP·Ar_n ($n = 1, 2$) clusters.[15] $(2AP)_2$ has been investigated as a mimetic model for excited-state reactions such as photoinduced single and double proton transfer along the H-bonds of doubly N−H···N bonded DNA base pairs. Sobolewski and Domcke have calculated the ground- and excited-state geometries for the normal, single H-atom and double-proton transfer forms and investigated the excited-state N−H stretching reaction path leading to H-atom transfer, at the CASSCF and multireference MP2 (MRMP2) levels.[6] Jet-cooled $(2AP)_n$ clusters were later investigated by femtosecond UV/UV pump−probe photoionization at excess vibrational energies of 2000−8200 cm^{-1} above the S_1 electronic origin.[9,10] A 50−70 ps excited-state deactivation process with a slightly nonmonotonic dependence on the excess vibrational energy was observed in the $(2AP)_2^+$ mass channel and was interpreted as reflecting the internal conversion from the $^1\pi\pi^*$ doorway state to a charge-transfer $^1\pi\pi^*$ state, accompanied by H-atom transfer.[9,10] Wu and Brutschy measured the infrared spectrum of $(2AP)_2$ over the range 3200−3600 cm^{-1} and observed two bands at 3319 and 3529 cm^{-1}, which they assigned to the H-bonded N−H_b and the free N−H_f stretching vibrations of the amino group (see also the scheme above).[8] Very recently, Yamada et al. have carried out picosecond IR/UV pump−probe measurements to elucidate vibrational energy relaxation of the N−H stretching vibrations of 2AP and $(2AP)_2$.[16] We have investigated 2AP paired to 2-pyridone (2PY) and have reported the intermolecular frequencies in the ground and first excited states[17] as well as the infrared spectrum.[7] In these studies, the 2-pyridone coun-

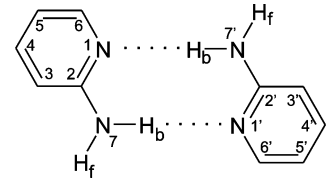

* To whom correspondence should be addressed. E-mail: leutwyler@iac.unibe.ch.

10.1021/jp811359k CCC: $40.75
Published on Web 04/09/2009

terpart served as a structural analogue for uracil or thymine, in order to mimic the adenine·uracil base pair.[7,17,18]

The previous studies of $(2AP)_2$ resulted in (or were based on) a single ground-state geometry of C_i symmetry,[3,6,8] and only this form was considered in subsequent spectroscopic and reaction dynamical investigations.[3,8−10,16] Due to the nonplanarity of the NH_2 group,[1] one expects that self-dimerization of 2AP results in distinct "up−up" and "up−down" conformers (as well as the respective "down−down" and "down−up" enantiomers). Here we present a combined ab initio computational and experimental study of the S_0 ground-state of $(2AP)_2$. Large basis set calculations at the MP2 and ΔCCSD(T) levels confirm the existence of two different conformers of C_i and C_2 symmetry; both are chiral, each giving rise to a pair of enantiomers. We have also reinvestigated the lowest electronic excitations of $(2AP)_2$, using mass-selective resonant two-photon ionization (R2PI) and UV/UV holeburning laser spectroscopies. The results reported below confirm contributions of two ground-state species to the optical spectrum. We have also remeasured the mass-selective infrared spectrum of $(2AP)_2$ over the extended 2600−3600 cm^{-1} range. Comparison to the IR spectra of 2PY·2AP dimer[7] and to the ab initio calculated frequencies of $(2AP)_2$ leads to a major reassignment of the infrared spectrum of $(2AP)_2$.[8,16]

II. Experimental and Computational Methods

A. Experimental Techniques. 2-Aminopyridine (Fluka, puriss.) was placed in a 20 Hz magnetically actuated pulsed nozzle and heated to 50 °C. The $(2AP)_2$ dimers were produced and cooled in a pulsed supersonic expansion through a thin-walled 0.6 mm diameter nozzle, using Ne carrier gas at a backing pressure of 1.6 bar. Two-color resonant two-photon ionization (2C-R2PI) and UV/UV depletion measurements were performed by overlapping the excitation laser with the ionization laser beam temporally and spatially within the source of a 1 m time-of-flight mass spectrometer (TOF), as described previously.[7,19] Electronic excitation of $(2AP)_2$ in the range 31 500−32 500 cm^{-1} was performed with a frequency doubled dye laser (100 μJ/pulse) pumped by the 532 nm output of an Nd:YAG laser. The electronically excited species were ionized with the 266 nm output (400 μJ/pulse) of the same Nd:YAG. For the UV/UV depletion experiments, the tunable burn laser (∼300 μJ/pulse) preceded the R2PI excitation/ ionization pulses by 300 ns. The burn laser was scanned and the remaining ground-state clusters probed by 2C-R2PI with the excitation laser at the respective 0_0^0 band. At the electronic origins, the ground-state population depletions were ∼70%.

Mass- and isotopomer-specific IR spectra were measured with the IR/UV double resonance method,[7,20−25] by overlapping the focused IR and the UV laser beams nearly collinearly in the source of the TOF-MS. The UV excitation laser energy was ∼500 μJ/pulse, in order to saturate the corresponding $S_1 \leftarrow S_0$ origin and minimize the R2PI signal fluctuations. Every other UV laser pulse was preceded by 100 ns with a spatially overlapped IR pulse generated by a 10 Hz LaserVision OPO/OPA system, which was mildly focused by a 1000 mm CaF_2 lens. When the IR laser frequency coincides with an IR transition out of the level being monitored, its ground-state population decreases and the R2PI signal originating from the same S_0 state level is depleted. The difference in the 2C-R2PI ion signal obtained without and with the IR laser present was recorded as a function of IR frequency. The signal was recorded shot-by-shot with a LeCroy digital oscilloscope and subsequently processed with a LabView program.

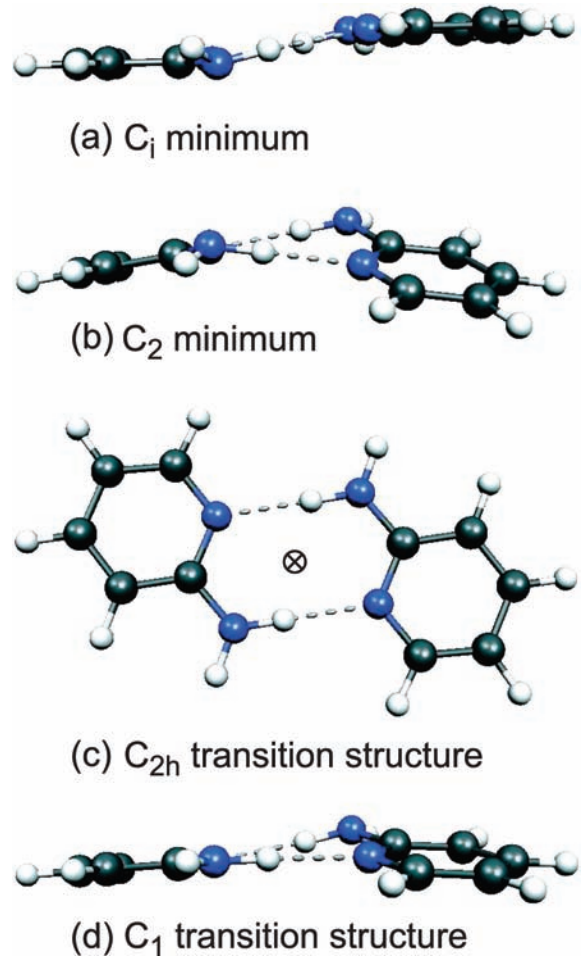

Figure 1. Geometries of (2-aminopyridine)$_2$, optimized at the MP2/aug-cc-pVQZ level of theory. (a) C_i minimum-energy structure, (b) C_2 minimum-energy structure, (c) C_{2h}-symmetric index-2 transition structure, (d) C_1 index-1 transition structure between C_2 and C_i; see Figure 2.

B. Computational Methods. The ground-state structure of $(2AP)_2$ was optimized using second-order Møller−Plesset perturbation theory (RI-MP2) with the aug-cc-pVXZ (X = D, T, Q) basis sets. The MP2 binding energies were then extrapolated to the complete basis set (CBS) limit using this basis set series and the extrapolation scheme proposed by Dunning and co-workers.[26] Higher order electron correlation contributions were evaluated at the CCSD(T) level, by calculating the ΔCCSD(T) correction term ($\Delta CCSD(T) = D_{e,CCSD(T)} - D_{e,MP2}$) with the aug-cc-pVDZ basis set.[27] Structure optimizations and vibrational calculations were also performed at the DFT level, using the PW91 and B3LYP functionals with the 6-311++G(d,p) basis set. Normal modes, harmonic vibrational frequencies, and zero-point vibrational energies of the two minimum-energy and two transition structures (discussed below) were calculated at the MP2/aug-cc-pVDZ, PW91, and B3LYP levels of theory. Anharmonic vibrational frequencies were also calculated with the B3LYP functional. The DFT and CCSD(T) calculations were carried out using Gaussian 03[28] and the RI-MP2 calculations with TURBOMOLE 5.9.[29]

III. Results and Discussion

A. Potential Energy Surface and Symmetry Aspects. Both MP2 and DFT geometry optimizations of $(2AP)_2$ yielded minimum-energy structures of C_i and C_2 symmetry; the former are shown in Figure 1a,b. The NH_2 group pyramidal angles are

TABLE 1: MP2/aug-cc-pVQZ Optimized Geometries of (2-Aminopyridine)$_2$, (2AP)$_2$, and the 2-Aminopyridine Monomer (2AP): Intramolecular Bond Lengths (r, Å), Intermolecular Distances (R, Å), Angles (θ, deg), Dihedral Angles (τ, deg), and Dipole Moments (D)

	(2AP)$_2$		
parameter	C_i	C_2	2AP
r(C−N$_{amino}$)	1.366	1.366	1.384
r(N−H$_b$)	1.022	1.022	1.007
r(N−H$_f$)	1.004	1.004	1.005
R(H···N)	1.978	1.977	
θ(C−N−H$_b$)	117.4	117.2	113.1
θ(C−N−H$_f$)	116.8	116.7	116.2
θ(N−H···N)	176.1	178.6	
τ(H$_b$−N−C−H$_f$)	145.3	144.6	134.5
dipole moment	0.0	1.25	2.01

opposite for the C_i and in the same direction for the C_2 dimer. Selected MP2/aVQZ geometry parameters for the two conformers and the 2AP monomer are given in Table 1. Apart from the different relative arrangement of the monomers, the structural differences between the two conformers are small: The N−H···N intermolecular distances agree to within 0.001 Å, indicating virtually identical hydrogen-bond strengths. In both conformers, the N−H···N hydrogen bonds deviate from linearity, by 3.9° for the C_i and by 1.4° for the C_2 conformer. The H$_b$−N−C−H$_f$ dihedral angles differ by 0.7°, the pyramidal character being slightly more pronounced in the C_2 symmetric conformer.

The conformers are calculated to be very close in energy. With the 6-311++G(d,p) basis set, both the PW91 and B3LYP functionals predict the C_i conformer to be the global minimum. The B3LYP C_i (but not the C_2) structure has been characterized by Wu and Brutschy.[8] In contrast, the MP2 optimizations with the aug-cc-pVXZ (X = D, T, Q) basis set series consistently predict larger binding energies for the C_2 conformer; this remains true upon CBS extrapolation of the binding energies and upon adding the ΔCCSD(T) correction. The MP2(CBS)+ΔCCSD(T) binding energies are D_e = 10.70 (C_i) and 10.72 (C_2) kcal/mol, respectively; see also Table 2.

By comparison, the B3LYP/6-311++G(d,p) binding energy of the C_i dimer is D_e = 9.29 kcal/mol,[8] about 1.4 kcal/mol smaller than the MP2(CBS)+ΔCCSD(T) values. This finding is in agreement with calculations of the binding energies of 10 different uracil dimers, where the B3LYP binding energies were between 1.4 and 2.1 kcal/mol smaller than the MP2(CBS)+ΔCCSD(T) binding energies.[30] The vibrational zero-point energy (ZPE) correction terms, calculated at the MP2/aug-cc-pVDZ level, are also very similar, +0.913 kcal/mol (C_i) and +0.901 kcal/mol (C_2), respectively. The final calculated dissociation energy of the C_2 conformer is D_0 = 9.815 kcal/mol, only 0.024 kcal/mol (8.4 cm^{-1}) larger than for the C_i conformer.

Both the C_2 and C_i conformers are chiral; hence, both exist as enantiomeric pairs. Altogether, this must lead to a 4-fold minimum potential energy surface (PES), which was investigated at the MP2 level with the cc-pVDZ basis set. Figure 2 shows the PES calculated along the H$_b$−N−C−H$_f$ and H′$_b$−N′−C′−H′$_f$ dihedral angle coordinates of each 2-aminopyridine monomer. These were stepped in increments of 10° up to ±80° and the remaining internal coordinates fully optimized for each pair of angles. Two types of transition structure can be identified in Figure 2: Each of the C_2 minima is connected to its two neighboring C_i minima via asymmetric (C_1) index-1 transition structures. The planar C_{2h} symmetric structure at the center of the graph, directly connecting the two C_2 and the two C_i minima, is an index-2 transition structure. Normal mode analysis at the C_{2h} stationary point at the MP2/aug-cc-pVDZ level yields two normal modes (a_u and b_g symmetry) with imaginary frequencies, shown in Figure 3. The a_u mode corresponds to the "butterfly" distortion from the C_{2h} point toward the C_2 minima. The b_g mode corresponds to the "twist" vibration pointing toward the two C_i minima. Both transition structures were optimized at the MP2/aug-cc-pVTZ level, and the CBS extrapolated energies and ΔCCSD(T)/6-31+G(d,p) corrections were calculated at these structures. The C_1 barrier height in the $C_2 \rightarrow C_i$ direction is 65 cm^{-1}. The planar C_{2h} symmetric transition structure is calculated to lie 126 cm^{-1} above the C_2 minimum, twice as high as the C_1 barrier. The interconversion between the respective enantiomers gives rise to vibrational states that are split by butterfly inversion tunneling (along β) or twist tunneling (along θ).

Sobolewski and Domcke have calculated the ground-state geometries of the C_i symmetric and planar C_{2h} forms at the MP2/6-31G(d,p) level.[6] With this much smaller basis set, the angles at the amino groups are less pyramidal and the N−H···N hydrogen bonds are 0.06 Å longer,[6] compared to the aug-cc-pVQZ geometry (see Table 1). Also, the C_{2h} structure is calculated to lie considerably higher, 436 cm^{-1} above the C_i form.[6]

The harmonic vibrational frequencies at the C_2 and C_i minima were calculated at the MP2/aug-cc-pVDZ level. On the basis of the sum of the vibrational zero-point energies of the low-frequency θ (propeller twist) and β (butterfly) modes (25−27 cm^{-1}), the C_1 barriers are high enough to stabilize the zero-point vibrational levels as well as the $v = 1$ levels of the θ and β vibrations of the C_2 and C_i forms. However, the higher θ and β levels lie above the C_i barriers and are delocalized over all four wells.

In summary, a correct description of the (2AP)$_2$ ground-state should encompass both the C_2 and C_i conformers, since these coexist down to low temperatures. Given the small energy difference, even the present calculations cannot definitively decide which conformer is more stable. Only the lowest few vibrational states are localized within the respective C_2 and C_i wells.

B. Resonant Two-Photon Ionization and UV/UV Depletion Spectroscopy. The unseparated two-color resonant two-photon ionization spectrum of (2AP)$_2$ is shown in the second trace of Figure 4. The main spectral features are generally in agreement with the one-color R2PI spectra of refs 3 and 8, although their spectra are typically less resolved, probably due to optical saturation of the vibronic bands. In agreement with refs 3 and 8, we assign an electronic origin at 31 808 cm^{-1}.

We note, however, that this is the $S_2 \leftarrow S_0$ origin, the lower-lying $S_1 \leftarrow S_0$ origin being very weak. Although the $S_1 \leftarrow S_0$ and $S_2 \leftarrow S_0$ transitions of (2AP)$_2$ and their excitonic coupling will be analyzed elsewhere, a brief discussion is necessary here. The ground-state of the C_i isomer transforms as A_g. In its lowest excited states, (2AP)$_2$ is planar and C_{2h} symmetric; the S_1 and S_2 states transform as A_g and B_u, respectively. Therefore, the $S_2 \leftarrow S_0$ transition is electric-dipole allowed, while the $S_1 \leftarrow S_0$ transition is strictly forbidden for the C_i isomer. For the ground-state C_2 isomer, the S_0 state transforms as A and the excited states as A_g (S_1) and B_u (S_2), as before. Again, the $S_2 \leftarrow S_0$ transition is fully allowed. Now, however, the $S_1 \leftrightarrow S_0$ transition is also weakly allowed, since the transition dipole moments of both monomers have a small additive projection onto the C_2 symmetry axis of the dimer. A very weak band attributable to the $S_1 \leftarrow S_0$ electronic origin is in fact visible 11 cm^{-1} below the strong $S_2 \leftarrow S_0$ origin in Figure 4 and is expanded in Figure 5.

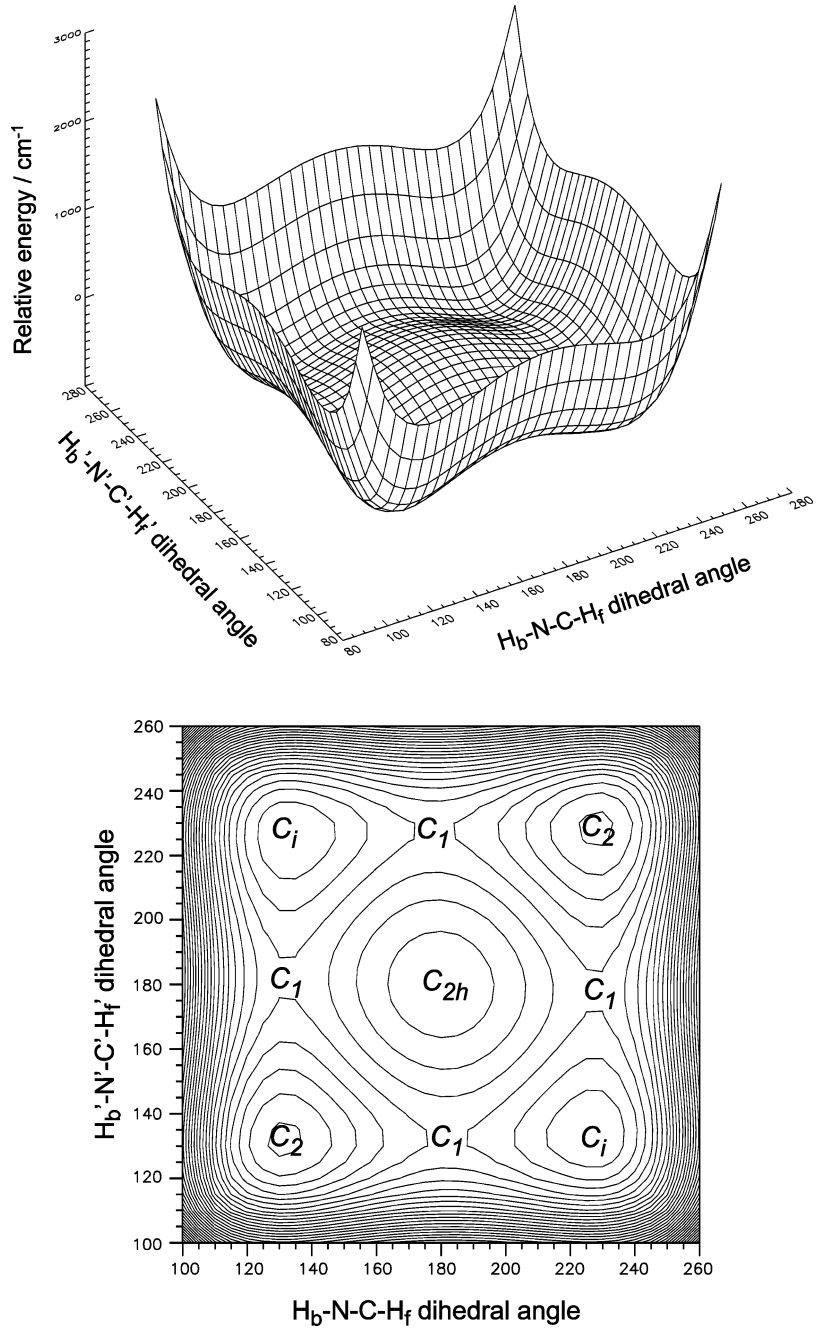

Figure 2. MP2/cc-pVDZ-calculated ground-state potential energy surface of (2-aminopyridine)$_2$. The energies (in cm^{-1}) are plotted as a function of the H−N−C−H dihedral angles, relative to the C_{2h} local maximum.

TABLE 2: Binding and Dissociation Energies (in kcal/mol) of the (2-Aminopyridine)$_2$ Stationary Points: C_i (relative Minimum), C_2 (absolute Minimum), C_{2h} (Transition Structure), and C_1 (Transition Structure), Based on MP2/aug-cc-pVTZ Optimized Geometries

	basis set	C_i	C_2	C_{2h} (TS)	C_1 (TS)
D_e(MP2)	CBS[a]	−11.134	−11.157	−10.819	−10.982
D_e + ΔCCSD(T)	6-31+G(d,p)	−10.755	−10.761	−10.402	−10.575
D_e + ΔCCSD(T)	aug-cc-pVDZ	−10.704	−10.717	−10.287	
ΔZPE[c]	aug-cc-pVDZ	+0.913	+0.901		
D_0[d]	CBS/aug-cc-pVDZ	−9.791	−9.815		

[a] Complete basis-set extrapolation; see ref 26. [b] ΔCCSD(T) = D_e[CCSD(T)] − D_e(MP2). [c] MP2 zero point energy correction. [d] D_0 = D_e(CBS) + ΔCCSD(T) + ΔZPE.

That this band is indeed the S_1←S_0 origin and not a sequence or hot band is demonstrated by lowering the dimer symmetry via isotopic substitution of a ^{12}C by a single ^{13}C atom. This substitution lowers the symmetry of the nuclear framework, from C_2 to C_1 in the ground-state and from C_{2h} to C_s in the excited state. This renders the S_1←S_0 transition of (2AP)$_2$-^{13}C isotopomer more strongly allowed than for the normal (2AP)$_2$: The band 11 cm^{-1} below the S_2 electronic origin in the mass-specific R2PI

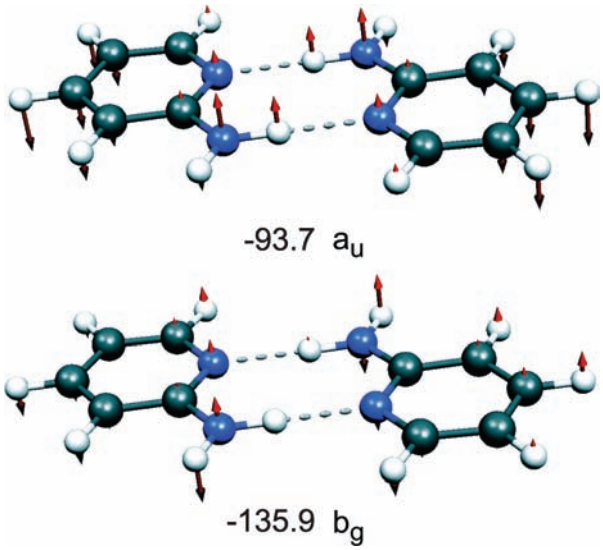

Figure 3. The a_u and b_g normal modes of the C_{2h} TS structure with imaginary frequencies. These connect the C_{2h} TS structure to the C_2 and C_i minima, respectively.

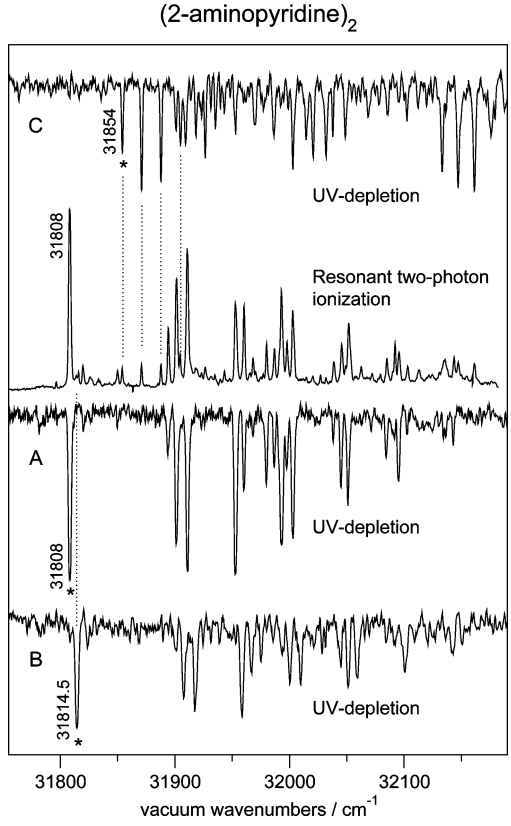

Figure 4. Two-color resonant two photon ionization spectra and UV/UV depletion spectra of species A−C, observed in the (2-aminopyridine)$_2^+$ ion channel. The bands used for detection of the UV/UV depletion spectra are marked by asterisks.

spectrum of (2AP)$_2$-^{13}C now has ∼15% of the intensity of the S_2 origin. This enhancement proves that this band is the S_1←S_0 electronic origin and gives the exciton splitting between the S_1/S_2 origins as $\Delta \sim 11$ cm^{-1}. An analogous ^{12}C/^{13}C isotopic substitution effect on the intensities of the excitonically coupled S_1 and S_2 states has been previously demonstrated for the 2-pyridone dimer, (2PY)$_2$.[31] A detailed treatment of the S_1/S_2 excitonic coupling including deuteration effects will be given elsewhere.

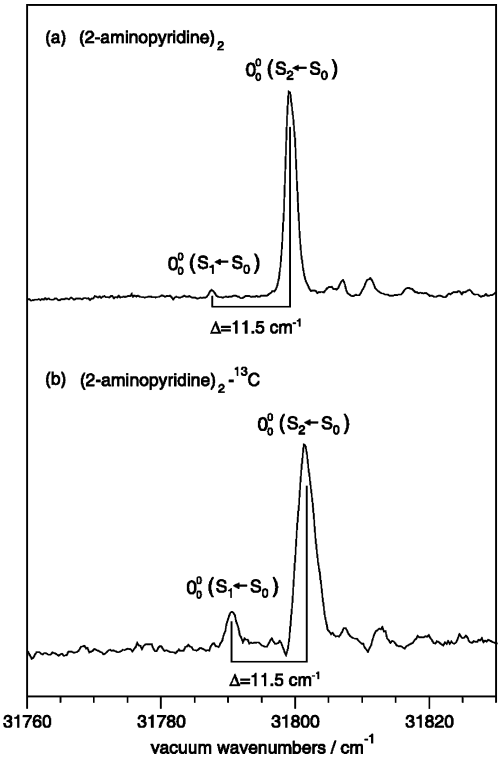

Figure 5. Two-color resonant two-photon ionization spectra of the origin regions of (a) (2-aminopyridine)$_2$ and (b) (2-aminopyridine)$_2$-^{13}C. Note the S_1/S_2 exciton splitting $\Delta = 11.5$ cm^{-1} and the intensity difference of the S_1←S_0 and S_2←S_0 electronic origin bands in part a compared to b, discussed further in the text.

A detailed comparison shows that while in the spectrum of ref 3 there is a weak band at 31 854 cm^{-1}, 46 cm^{-1} above the origin, in our spectrum this band is followed by two more bands at 62 and 78 cm^{-1}, i.e., spaced by 16 cm^{-1}. Comparing Figure 4 to the one-color R2PI spectrum of ref 8 one finds that the weak bands at 46, 62, and 78 cm^{-1} are about 4 times more intense in their spectrum. These differences between the three spectra strongly suggest the existence of different ground-state species with relative populations depending on the expansion conditions.

Using UV/UV depletion spectroscopy with selective detection at three different bands in the R2PI spectrum, we have been able to separate spectra of *three* different ground-state species. Detection at the lowest-frequency intense band at 31 808 cm^{-1} gives rise to the UV depletion spectrum shown in Figure 4A. This species contributes the major part to the R2PI spectrum. Detection at the weak band at 31 814.5 cm^{-1} (6.5 cm^{-1} above the origin) gives rise to the depletion spectrum shown in Figure 4B. This is a minor contribution to the R2PI spectrum, with a Franck−Condon pattern that is very similar to species A, but with all the bands shifted by 5−6 cm^{-1} to the blue. Detection at the band 46 cm^{-1} higher (31 854 cm^{-1}) gives rise to the depletion spectrum shown as Figure 4C. The vibronic progressions of this species are very different from that of conformers A and B. Together, these three contributions sum up to the observed two-color R2PI spectrum.

The UV spectrum of species A is assigned as originating from the vibrational ground-state of the C_2 symmetric conformer. The assignments rest on (i) the calculations discussed above; (ii) the fact that the S_1←S_0 electronic origin is weakly observed (see above), which is only possible for the C_2 isomer; and (iii) the infrared spectrum discussed below. The vibronic spectra of A and B are very similar, with vibrational fundamentals in the 90

and 140 cm^{-1} range, assigned to the excited-state intermolecular shear (χ') and stretch (σ') modes. The interaction of the latter two vibrations with the excitonically coupled S_1 and S_2 states gives rise to complex splitting patterns for these bands. These details of the R2PI spectrum will be discussed elsewhere.

Species B is assigned as originating from the lowest vibrational level of the C_i symmetric conformer. Figure 2 shows that the C_i isomer can be viewed as a "hot" level of the C_2 isomer, albeit one that is localized in the higher C_i well pair. In a sense, this absorption could be called a "hot" band. Due to the low $C_2 \rightarrow C_i$ barrier of 60 cm^{-1}, the conformer populations are expected to be determined by the vibrational temperature in the supersonic jet. Assuming that the energy difference between the two isomers is given by the difference of the MP2/ΔCCSD(T) calculated D_0 values of 8.4 cm^{-1} and assuming a vibrational temperature $T_{vib} = 5$ K in the molecular beam, the C_2/C_i population ratio should be ~11, in acceptable agreement with the experimental ratio of 14 for these two bands; see Figure 4.

The electronic origin of C at 31 854 cm^{-1} is shifted by 46 cm^{-1} to the blue of the electronic origin of A. It exhibits an extended progression in a low-frequency mode of 16 cm^{-1}. On the basis of their IR depletion spectra, Wu and Brutschy assigned the UV bands of C to the same species as A, claiming to have found no indication for another isomer;[8] this does not agree with the present finding. Investigation of the 2C-R2PI spectrum of the trimer mass channel $(2AP)_3^+$ shows no signal corresponding to this band system. In agreement with Hager et al.,[3] we observe that the contribution of C to the spectrum is temperature-dependent. Much more significantly, however, it depends on the H_2O vapor content of the carrier gas. On the basis of this observation and the IR depletion spectrum of C discussed below, we propose that C is the monohydrate cluster, $(2AP)_2 \cdot H_2O$, that appears by efficient dissociation of the $(2AP)_2 \cdot H_2O^+$ ion into the $(2AP)_2^+$ mass channel.

C. Infrared-Depletion Spectra and Intramolecular Vibrations in the Hydride Stretching Region. The IR/UV depletion spectra of the species A−C observed in the $(2AP)_2^+$ ion channel are shown in Figure 6. Analogous to the observations in the R2PI and UV/UV depletion spectra above, the IR spectra of species A and B are very similar, while that of C is very different. Comparing the IR/UV depletion spectra of species A and B, a slight shift (2 cm^{-1}) of the free N−H stretch of species B to lower wavenumbers is observed. Given the lower signal-to-noise ratio of spectrum B, there are no other significant differences. In order to simplify the discussion, we refer below to the IR spectrum of species A as "the" $(2AP)_2$ IR spectrum.

We first consider the assignment of the $(2AP)_2$ spectrum: In Figure 7 we show the IR/UV spectra in the 2600−3600 cm^{-1} range of (a) the 2-pyridone self-dimer, $(2PY)_2$, first measured in ref 32, (b) 2-pyridone·2-aminopyridine,[7] and (c) (2-aminopyridine)$_2$. Schemes of the corresponding structures are given as insets. The experimental frequencies of $(2PY)_2$, 2AP·2PY, $(2AP)_2$, and the 2AP monomer are summarized in Table 3. The IR spectrum of $(2PY)_2$ shows an extremely broad and slightly structured band extending from 2700 to 3050 cm^{-1}. The oscillator strength of this band arises from the N−H stretches, and the extreme broadening is probably due to anharmonic coupling with the H−N−C=O bend overtones. The spectrum of 2PY·2AP dimer also shows a broad low-frequency region between 2700 and 2900 cm^{-1} characteristic for the 2PY N−H stretch. However, compared to the $(2PY)_2$ spectrum, this region is now more sharply structured and ~150 cm^{-1} narrower. In addition, three sharp bands appear at 3139, 3320, and 3533 cm^{-1}. On the basis of partial and full H/D substitution, these

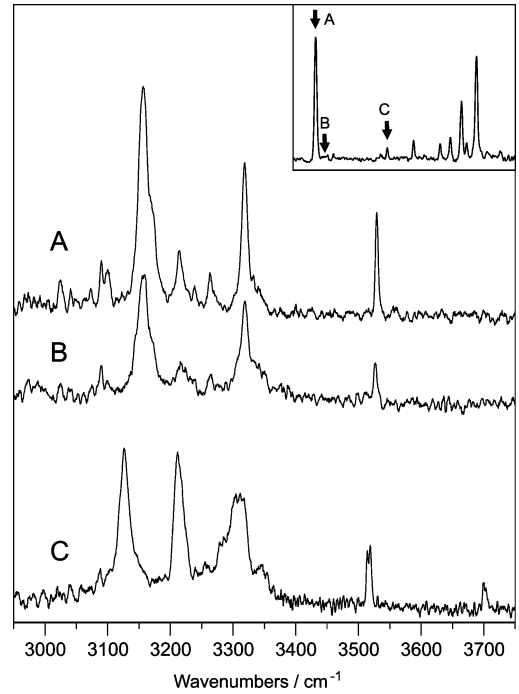

Figure 6. Infrared−ultraviolet depletion spectra of species A−C, recorded at the bands indicated in the inset.

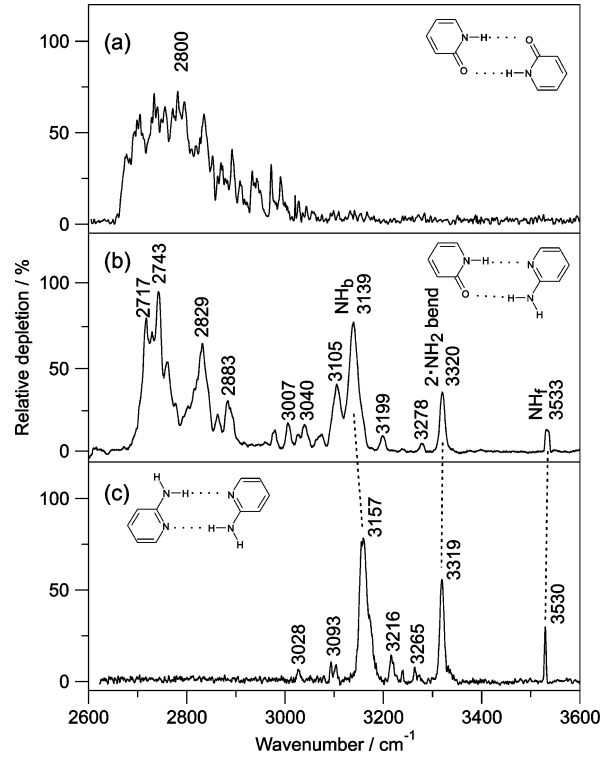

Figure 7. Comparison of the experimental IR/UV depletion spectra of (a) $(2\text{-pyridone})_2$, (b) 2-pyridone·2-aminopyridine, and (c) $(2\text{-aminopyridine})_2$; see Figure 6a.

have been previously assigned to the bound N−H_b stretch, the overtone of the H−N−H amino group bend, and to the free N−H_f stretch, respectively; see also Table 3.[7]

The $(2AP)_2$ spectrum exhibits three sharp bands at 3157, 3319, and 3530 cm^{-1}, in close proximity and with similar intensities to those of the 2PY·2AP dimer. The close similarity of the two IR spectra allows a straightforward assignment of the bands in the $(2AP)_2$ spectrum to the bound N−H_b stretch, the NH_2 bend

TABLE 3: Experimental Infrared Frequencies (cm^{-1}) and Band Assignments for (2-Aminopyridine)$_2$ [(2AP)$_2$], 2-Pyridone·2-Aminopyridine (2PY·2AP), (2-Pyridone)$_2$ [(2PY)$_2$], and 2-Aminopyridine

	(2AP)$_2$	2PY·2AP	(2PY)$_2$	2-aminopyridine[a]	
N−H$_f$ stretch	3530	3533	−	antisym NH_2 stretch	3546
2·H−N−H bend	3319	3320	−		−
C_5−H stretch	3216				
N−H$_b$ stretch	3157	3139	−	sym NH_2 stretch	3439
$C_{3,4}$−H stretch	3103				
$C_{3,4}$−H stretch	3093				
C_6−H stretch	3028				
2PY N−H stretch	−	2717−2900	2700−3050		

[a] 2-Aminopyridine·Ar; see ref 8.

TABLE 4: Calculated PW91 Harmonic and B3LYP Anharmonic Vibrational Frequencies (in cm^{-1}) and Infrared Intensities (km/mol, in parentheses) of the C_2 and C_i Symmetric Conformers of (2-Aminopyridine)$_2$, Using the 6-311++G(d,p) Basis Set

	C_2 conformer			C_i conformer		
description	irrep	PW91 harmonic	B3LYP anharmonic[a]	irrep	PW91 harmonic	B3LYP anharmonic[a]
N−H$_f$ stretch	b	3608.7 (90.0)	3521.1 (112.7)	a_u	3606.3 (89.3)	3526.2 (112.7)
N−H$_f$ stretch	a	3608.4 (0.0)	3520.8 (0.0)	a_g	3605.9 (0.0)	3525.8 (0.0)
2·H−N−H bend	b	3305.6	3350.7	a_u	3303.7	3353.2
2·H−N−H bend	a	3308.2	3321.9	a_g	3305.6	3322.6
2·H−N−H bend	a	3303.0	3303.0	a_u	3301.8	3303.8
C_5−H stretch	b	3143.4 (19.0)	3070.7 (28.2)	a_u	3143.4 (23.9)	3059.7 (28.4)
C_5−H stretch	a	3143.2 (0.1)	3070.5 (0.3)	a_g	3143.2 (0.0)	3059.5 (0.0)
$C_{3,4,5}$-H stretch	b	−	3053.0 (39.5)	a_u	−	3043.1 (39.4)
N−H$_b$ stretch	b	3121.0 (1015)	−	a_u	3122.3 (2000)	−
$C_{3,4,5}$-H stretch	a	3119.5 (0.0)	3057.3 (0.0)	a_g	3119.4 (0.0)	3047.0 (0.0)
N−H$_b$ stretch	b	3116.6 (2323)	3074.5 (2292.9)	a_u	3117.9 (1313)	3036.1 (2277)
$C_{3,4}$−H stretch	a	3103.3 (0.2)	3027.7 (0.2)	a_g	3103.3 (0.0)	3016.4 (0.0)
$C_{3,4}$−H stretch	b	3102.9 (6.3)	3028.8 (12.2)	a_u	3102.9 (6.3)	3017.8 (12.5)
C_6−H stretch	a	3076.1 (0.0)	2988.1 (0.2)	a_g	3077.1 (0.0)	2982.3 (0.0)
C_6−H stretch	b	3072.3 (157)	2991.7 (48.6)	a_u	3072.5 (144.0)	2977.9 (48.4)
N−H$_b$/C−H stretch	a	3064.7 (0.7)	3053.9 (1.2)	a_g	3067.4 (0.0)	3063.1 (0.0)
H−N−H bend	a	1654.1 (0.0)		a_g	1652.8 (0.0)	
H−N−H bend	b	1651.5 (465)		a_u	1650.9 (464)	

[a] IR intensities taken from the harmonic B3LYP6-311++G(d,p) calculation.

overtone, and the free N−H$_f$ stretch, respectively; see also Table 3. For the free N−H$_f$ stretch and the NH_2 bend overtone, the wavenumbers agree with those of 2PY·2AP within ∼1−2 cm^{-1}, as would be expected for vibrations that mainly involve atoms that are *not* H-bonded. The bound N−H$_b$ stretch is 21 cm^{-1} *less* red-shifted than its 2PY·2AP counterpart, which is expected, since the N−H···N hydrogen bond in (2AP)$_2$ is weaker than the N−H···O═C hydrogen bond in 2PY·2AP.[7] The weaker bands in the (2AP)$_2$ spectrum at 3028, 3093, 3103, and 3216 cm^{-1} are assigned to C−H stretches, in agreement with the PW91-calculated IR frequencies and intensities given in Table 4. Note that almost all vibrations of the C_2 (C_i) symmetric conformers occur as pairs of symmetric and antisymmetric frequencies. Due to the IR selection rules for C_2/C_i species, the allowed transitions are the antisymmetric ones (b/a_u).

Frequency stick plots calculated at the PW91/6-311++G(d,p), RI-MP2/aVDZ, as well as the harmonic and anharmonic B3LYP/6-311++G(d,p) levels for the C_2 minimum structure are compared to the experimental IR spectrum in Figure 8. The harmonic PW91 and the anharmonic B3LYP vibrational frequencies are in good agreement with the experiment for the H−N−H bend overtone and the free N−H stretch. The bound N−H$_b$ stretch is calculated somewhat too low by both methods. In contrast, the RI-MP2/aVDZ as well as the harmonic B3LYP calculations strongly overestimate the vibrational frequencies, particularly those of the bound N−H stretch modes; see Figure 8c,d. Agreement can be improved by applying frequency scaling factors, as in ref 8. The scaled MP2 and harmonic B3LYP spectra are shown in Figure 8c,d. However, the agreement of the scaled spectra is inferior to both the harmonic PW91 and anharmonic B3LYP calculated IR spectra.

Returning to the IR spectrum of species C, a crucial difference relative to the IR spectra of A and B (Figure 6) is the sharp band at 3702 cm^{-1} which cannot be interpreted in terms of N−H stretches. On the other hand, it is characteristic for a free OH stretch vibration, implying that species C might be the (2AP)$_2$·H$_2$O complex that fragments upon ionization. In Figure 9 we compare the IR/UV spectrum of species C to the IR spectra of three energetically low-lying H-bonded structures of (2AP)$_2$·H$_2$O, calculated at the PW91/6-311++G(d,p) level.

The best agreement of the calculation with the experimental IR spectrum is found for a C_2-type structure with the H_2O inserted into one of the N−H···N hydrogen bonds; see Figure 9, panel 2. The bound O−H$_b$ vibration is shifted down to 3126 cm^{-1} (calculated at 3000 cm^{-1}). The asymmetry in the H-bond network introduced by the H_2O molecule gives rise to a splitting of the bound N−H$_b$ stretches to 3213 and 3270 cm^{-1}. The higher-frequency H-bonded N−H$_b$ stretch is assigned to the band at 3270 cm^{-1}, which overlaps with the NH_2 bend overtones at 3000−3010 cm^{-1}. The free N−H$_f$ stretch frequencies are shifted only slightly to 3516 cm^{-1} and are split by 3 cm^{-1}. Finally, the O−H$_f$ stretch is the highest band in the spectrum at 3702 cm^{-1}. Although a definitive assignment of the IR spectrum would need further investigations, the number and frequencies of the predicted bands is compatible with the observed spectrum. The

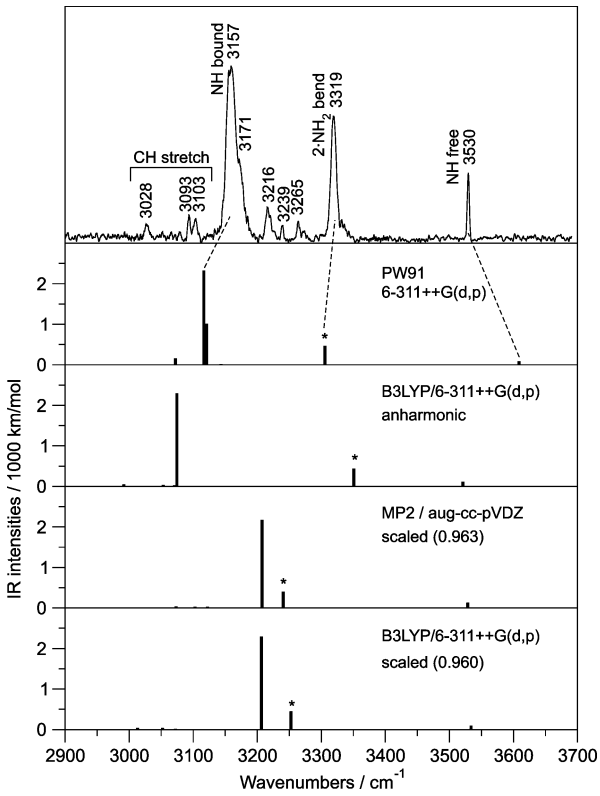

Figure 8. Comparison of the (2-aminopyridine)$_2$ experimental IR/UV depletion spectrum with the calculated vibrational frequencies of the C_2 isomer: (a) PW91/6-311++G(d,p), (b) anharmonic B3LYP/6-311++G(d,p), (c) harmonic RI-MP2/aVDZ (scaled by 0.963), and (d) harmonic B3LYP/6-311++G(d,p) (scaled by 0.960).

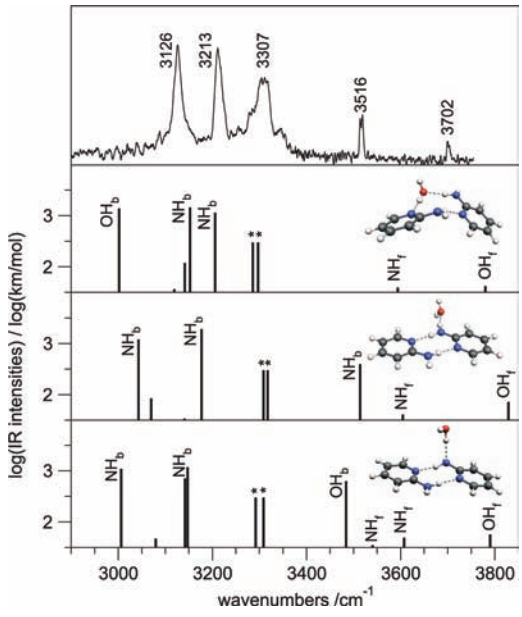

Figure 9. Comparison of the (2AP)$_2$·H$_2$O experimental IR/UV depletion spectrum to the PW91/6-311++G(d,p)-calculated frequency spectrum, for the three isomer structures that are shown as insets.

two other energetically low-lying alternative structures shown in panels 3 and 4 of Figure 9 each give rise to an intense calculated IR band that is not observed in the experimental spectrum, i.e., the N−H$_b$ and O−H$_b$ transitions calculated at ∼3500 cm^{-1}, respectively.

IV. Conclusions

Correlated calculations of the 2-aminopyridine dimer, (2AP)$_2$, at the MP2 level using the aug-cc-pVXZ (X = D, T, Q) basis sets, complete basis set extrapolations, and ΔCCSD(T) corrections establishes the existence of nearly degenerate conformers of C_2 and C_i symmetry. Their calculated binding energies D_e are 10.70 and 10.72 kcal/mol and their dissociation energies D_0 = 9.79 and 9.82 kcal/mol, respectively. The latter are ∼2 kcal/mol larger than that previously calculated by the B3LYP density functional method.[8] The energy difference between the C_i and C_2 conformers is 8 cm^{-1} in favor of the C_2 species, suggesting that both conformers may be observed down to very low temperatures. Both conformers are chiral, each giving rise to a pair of enantiomers. Calculation of the electronic ground-state surface along the amino flip coordinates shows two C_2 and two C_i minima, separated by four barriers of ∼65 cm^{-1}.

The R2PI and UV/UV depletion spectra of (2AP)$_2$ show separate contributions from distinct ground-state isomers (A and B) that are very similar. Assuming that A and B are in thermal equilibrium at T_{vib} ∼ 5 K in the supersonic beam and using the calculated 8 cm^{-1} energy difference, the observed intensity ratio in the R2PI spectrum agrees with the assignment of A as the C_2 and B as the C_i conformer. The IR/UV depletion spectra of A and B are also very similar. On the basis of the previous IR band assignments for 2AP·2-pyridone and on the calculated IR spectra of (2AP)$_2$, all major IR bands were assigned. The intense band at 3157 cm^{-1} is identified as the antisymmetric H-bonded N−H$_b$ stretch. The 3319 cm^{-1} band that was previously assigned to the N−H stretch[8,16] is reassigned to the overtone of the H−N−H bend. The previous assignment of the sharp band at 3530 cm^{-1} to the antisymmetric free N−H stretch[8,16] is confirmed. Several weaker C−H stretch fundamentals are also observed and assigned.

With respect to the picosecond IR/UV measurements of intramolecular vibrational relaxation (IVR) and vibrational predissociation of (2AP)$_2$ by Yamada et al.,[16] we note that the relaxation times measured for the band at 3221 cm^{-1} refer to the H−N−H bend overtone and not (as believed)[16] to the H-bonded N−H stretch. It will be interesting to measure the relaxation for the true N−H stretch band, as vibrational predissociation of (2AP)$_2$ should not be possible at 3157 cm^{-1} according the calculated CCSD(T) dissociation energies.

A third species (C) observed in the R2PI spectrum was separated by UV/UV holeburning. Its UV spectrum is qualitatively different those of A and B, with multiple 18 cm^{-1} progressions. The relative signal intensity of this species rises when adding H$_2$O to the carrier gas. Its IR/UV spectrum is assigned to the cluster (2AP)$_2$·H$_2$O, based on a characteristic "free" OH stretch at 3702 cm^{-1} and on the agreement with calculated IR spectra.

Finally, we note that the optical spectrum of (2AP)$_2$ not only exhibits contributions due to the C_2 and C_i isomers but also clear signatures of the excitonic coupling of the $S_1 \leftarrow S_0$ and $S_2 \leftarrow S_0$ electronic excitations, similar to that of the symmetric (2PY)$_2$ self-dimer.[31] A detailed treatment of these vibronic couplings will be given elsewhere.

Acknowledgment. We thank Mathias Weiss and Dr. A. Müller for their early contributions to this work. Financial support by the Schweiz. Nationalfonds (projects 113798 and 121993) is gratefully acknowledged.

References and Notes

(1) Kydd, R. A.; Mills, I. M. *J. Mol. Spectrosc.* **1972**, *42*, 320.
(2) Hager, J.; Wallace, S. *J. Phys. Chem.* **1985**, *89*, 3833.

(3) Hager, J.; Leach, G. W.; Demmer, D. R.; Wallace, S. *J. Phys. Chem.* **1987**, *91*, 3750.
(4) Borst, D. R.; Roscioli, J. R.; Pratt, D. W. *J. Phys. Chem. A* **2002**, *106*, 4022.
(5) Roscioli, J. R.; Pratt, D. W. *Proc. Natl. Acad. Sci. U.S.A.* **2003**, *100*, 13752.
(6) Sobolewski, A. L.; Domcke, W. *Chem. Phys.* **2003**, *294*, 73.
(7) Frey, J. A.; Müller, A.; Frey, H.-M.; Leutwyler, S. *J. Chem. Phys.* **2004**, *121*, 8237.
(8) Wu, R.; Brutschy, B. *J. Phys. Chem. A* **2004**, *108*, 9715.
(9) Schultz, T.; Samoylova, E.; Radloff, W.; Hertel, I. V.; Sobolewski, A. L.; Domcke, W. *Science* **2004**, *306*, 1765.
(10) Samoylova, E.; Smith, V. R.; Ritze, H.-H.; Radloff, W.; Kabelac, M.; Schultz, T. *J. Am. Chem. Soc.* **2006**, *128*, 15652.
(11) Hager, J.; Wallace, S. *J. Phys. Chem.* **1984**, *88*, 5513.
(12) Wallace, S. *J. Phys. Chem.* **1985**, *86*, 2218.
(13) Lin, J. L.; Wu, R. H.; Tseng, W. B. *Chem. Phys. Lett.* **2002**, *353*, 55.
(14) Baek, S. J.; Choi, K.-W.; Choi, Y. S.; Kim, S. K. *J. Chem. Phys.* **2002**, *117*, 2131.
(15) Baek, S. J.; Choi, K.-W.; Choi, Y. S.; Kim, S. K. *J. Phys. Chem. A* **2003**, *107*, 4826.
(16) Yamada, Y.; Mikami, N.; Ebata, T. *Proc. Natl. Acad. Sci.U.S.A.* **2008**, *105*, 12690.
(17) Müller, A.; Talbot, F.; Leutwyler, S. *J. Am. Chem. Soc.* **2002**, *124*, 14486.
(18) Roscioli, J. R.; Pratt, D. *Proc. Natl. Acad. Sci.U.S.A.* **2003**, *100*, 13752.
(19) Frey, J. A.; Leist, R.; Tanner, C.; Frey, H. M.; Leutwyler, S. *J. Chem. Phys.* **2006**, *125*, 114308.
(20) Page, R. H.; Shen, Y. R.; Lee, Y. T. *J. Chem. Phys.* **1988**, *88*, 4621.
(21) Riehn, C.; Lahmann, C.; Wassermann, B.; Brutschy, B. *Chem. Phys. Lett.* **1992**, *197*, 443.
(22) Pribble, R. N.; Hagemeister, F. C.; Zwier, T. S. *J. Chem. Phys.* **1997**, *106*, 2145.
(23) Yoshino, R.; Hashimoto, K.; Omi, T.; Ishiuchi, S.; Fujii, M. *J. Phys. Chem. A* **1998**, *102*, 6227.
(24) Matsumoto, Y.; Ebata, T.; Mikami, N. *J. Chem. Phys.* **1998**, *109*, 6303.
(25) Buchhold, K.; Reimann, B.; Djafari, S.; Barth, H.-D.; Brutschy, B.; Tarakeshwar, P.; Kim, K. S. *J. Chem. Phys.* **1999**, *110*, 8501.
(26) Dunning, T. H. *J. Chem. Phys.* **1989**, *90*, 1007.
(27) Hobza, P.; Šponer, J. *J. Am. Chem. Soc.* **2002**, *124*, 11802.
(28) Frisch, M. J.; Trucks, G. W.; Schlegel, H. B.; et al. *Gaussian 03, Rev. B.03*; Gaussian Inc.: Pittsburgh, PA, 2003.
(29) Ahlrichs, R.; Bär, M.; Häser, M.; Horn, H.; Kölmel, C. *Chem. Phys. Lett.* **1989**, *162*, 165 (current version: http://www.turbomole.de).
(30) Frey, J. A.; Müller, A.; Losada, M.; Leutwyler, S. *J. Phys. Chem. B* **2007**, *111*, 3534.
(31) Müller, A.; Talbot, F.; Leutwyler, S. *J. Chem. Phys.* **2002**, *116*, 2836.
(32) Matsuda, Y.; Ebata, T.; Mikami, N. *J. Chem. Phys.* **1999**, *110*, 8397.

JP811359K